Nat Hazards (2013) 69:749–779
DOI 10.1007/s11069-013-0728-5

ORIGINAL PAPER

Landslide susceptibility mapping by binary logistic regression, analytical hierarchy process, and statistical index models and assessment of their performances

H. R. Pourghasemi · H. R. Moradi · S. M. Fatemi Aghda

Received: 31 October 2012 / Accepted: 12 May 2013 / Published online: 25 May 2013

Abstract The current research presents a detailed landslide susceptibility mapping study by binary logistic regression, analytical hierarchy process, and statistical index models and an assessment of their performances. The study area covers the north of Tehran metropolitan, Iran. When conducting the study, in the first stage, a landslide inventory map with a total of 528 landslide locations was compiled from various sources such as aerial photographs, satellite images, and field surveys. Then, the landslide inventory was randomly split into a testing dataset 70 % (370 landslide locations) for training the models, and the remaining 30 % (158 landslides locations) was used for validation purpose. Twelve landslide conditioning factors such as slope degree, slope aspect, altitude, plan curvature, normalized difference vegetation index, land use, lithology, distance from rivers, distance from roads, distance from faults, stream power index, and slope-length were considered during the present study. Subsequently, landslide susceptibility maps were produced using binary logistic regression (BLR), analytical hierarchy process (AHP), and statistical index (SI) models in ArcGIS. The validation dataset, which was not used in the modeling process, was considered to validate the landslide susceptibility maps using the receiver operating characteristic curves and frequency ratio plot. The validation results showed that the area under the curve (AUC) for three mentioned models vary from 0.7570 to 0.8520 ($AUC_{AHP} = 75.70\ \%$, $AUC_{SI} = 80.37\ \%$, and $AUC_{BLR} = 85.20\ \%$). Also, plot of the frequency ratio for the four landslide susceptibility classes of the three landslide

H. R. Pourghasemi · H. R. Moradi (✉)
Department of Watershed Management Engineering, College of Natural Resources and Marine Sciences, Tarbiat Modares University (TMU), Noor, Mazandaran, Iran
e-mail: hrmoradi1340@yahoo.com; hrmoradi@modares.ac.ir

H. R. Pourghasemi
e-mail: hamidreza.pourghasemi@yahoo.com; hm_porghasemi@spatialacademy.com

S. M. Fatemi Aghda
Department of Engineering Geology, Tarbiat Moallem University (Kharazmi University), Tehran, Iran

S. M. Fatemi Aghda
The Ministry of Road and Urban Development (Road, Housing and Urban Development Research Center), Tehran, Iran

susceptibility models was validated our results. Hence, it is concluded that the binary logistic regression model employed in this study showed reasonably good accuracy in predicting the landslide susceptibility of study area. Meanwhile, the results obtained in this study also showed that the statistical index model can be used as a simple tool in the assessment of landslide susceptibility when a sufficient number of data are obtained.

Keywords Landslide susceptibility mapping · Binary logistic regression · AHP · Statistical index · North of Tehran · Iran

1 Introduction

In recent years, growing population and development of settlement, infrastructures, and life-lines have largely increased the impact of natural hazards both in industrialized and developing countries (Guzzetti 2005). Landslides play an important role in the evolution of landforms and represent a serious hazard in many areas of the World (Guzzetti 2005). In many countries, landslides generate large annual losses of property than any other type of natural hazards, including earthquakes, floods, and windstorms (Garcia-Rodriguez et al. 2008). According to Centre for Research on the Epidemiology of Disasters (CRED 2009), landslides accounted for approximately 4.4 % of natural disasters worldwide from 1990 to 2009, with 2.3 % of reported landslides occurring in Asia. To minimize the losses of human life and economic value, potential landslide-prone areas should be identified (Devkota et al. 2013). For this reason, landslide susceptibility maps may be helpful for planners, decision makers, and engineers in slope management and land use planning. A landslide susceptibility map gives an important indication of where future landslides are likely to occur based on the identification of areas of past landslide occurrences and areas where similar or identical physical characteristics exist (van Westen et al. 2006). Several different methods and techniques for landslide susceptibility mapping have been proposed and tested. However, no general agreement exists either on the methods for or on the scope of producing landslide susceptibility maps (Carrara et al. 1995; Soeters and van Westen 1996; van Westen et al. 1997; Aleotti and Chowdhury 1999; Guzzetti et al. 1999).

Many studies have evaluated landslide susceptibility using geographic information system (GIS) technology, and many of these studies have used probabilistic models (Lee and Pradhan 2006; Dahal et al. 2008; Oh et al. 2009; Ozdemir 2009; Yilmaz 2010; Oh and Lee 2011; Demir et al. 2012; Pourghasemi et al. 2012a, b; Mohammady et al. 2012; Xu et al. 2012c). The statistical index model is one of the bivariate models while were used by some researchers (Van Westen 1997; Rautela and Lakhera 2000; Cevik and Topal 2003; Tien Bui et al. 2011a; Raman and Punia 2012; Regmi et al. 2013). Also, several studies have been applied to assess landslide susceptibility using logistic regression models in different parts of the world (Ayalew and Yamagishi 2005; Lee and Pradhan 2007; Bai et al. 2010; Nandi and Shakoor 2010; Oh and Lee 2010; Ercanoglu and Temiz 2011; Erner and Duzgun 2012; Devkota et al. 2013).

The analytical hierarchy process and its combinations such as multi-criteria evaluation (MCE), multi-criteria decision analysis (MCDA), spatial multi-criteria evaluation (SMCE) have been used by different authors in landslide susceptibility mapping (Barredo et al. 2000; Nie et al. 2001; Ayalew et al. 2005; Komac 2006; Yalcin 2008; Akgun and Turk 2010; Pourghasemi et al. 2012c; Demir et al. 2012; Hasekiogullari and Ercanoglu 2012; Feizizadeh and Blaschke 2012a, b; Pourghasemi et al. 2012e).

In the past decade, some new methods such as artificial neural networks (ANNs) (Lee et al. 2004; Pradhan and Buchroithner 2010; Zare et al. 2012), fuzzy logic (Pradhan 2010a, b; Pradhan 2011a, b; Akgun et al. 2012; Pourghasemi et al. 2012c), and adaptive neuro-fuzzy inference system (ANFIS) (Vahidnia et al. 2010; Oh and Pradhan 2011; Sezer et al. 2011; Tien Bui et al. 2011b; Pradhan 2013) have been proposed.

Recently, new landslide susceptibility assessment methods such as support vector machine (SVM) (Ballabio and Sterlacchini 2012; Marjanović et al. 2011; Yao et al. 2008; Yilmaz 2010; Xu et al. 2012b; Pourghasemi et al. 2013), decision tree methods (Nefeslioglu et al. 2010; Tien Bui et al. 2012), index of entropy (Bednarik et al. 2010; Constantin et al. 2011; Pourghasemi et al. 2012d, f; Devkota et al. 2013; Wan 2012), Bayesian network (Song et al. 2012; Tien Bui et al. 2012), and fractal theory (Majtan et al. 2002; Yang and Lee 2006; Li et al. 2011) were tried, and their performances were assessed.

The main goals of the current research are to present a detailed landslide susceptibility mapping study by binary logistic regression, analytical hierarchy process, and statistical index models in a landslide-prone area (north of Tehran, Iran), and to assess their performances. The main difference between the present study and the approaches described in the aforementioned publications is to compare the performances of two statistical approaches such as bivariate and multivariate with an expert knowledge-based model (AHP) in landslide susceptibility mapping in the north of Tehran metropolitan, Iran.

2 Study area

The study area is located in the north of Tehran metropolitan, Iran, between longitudes 51°05′26″E and 51°50′30″E, and latitudes 35°45′50″N and 35°59′16″N (Fig. 1). It covers an area of about 900 km^2. Based on geological survey of Iran (GSI 1997), the lithology of study area is very variety and 33.97 % it covers by group 5 (Table 1) including alternation of shale and tuffaceous siltstone (E_3^{ss}), green crystal, lithic and ash tuff, tuff breccia, and partly with intercalations of limestone (E_2^{t}), alternation of shale and tuffaceous siltstone (E_2^{ts}), rhyolitic tuff with some intercalations of shale (E_2^{r}), massive green tuff, shale with dacitic and andesitic-basaltic lava flows (E_1^{tsv}), dark gray shale with alternation of green tuff, and partly with sandstone, shale, conglomerate and limestone (E_1^{sht}), alternation of green tuff and shale (E_1^{tsh}), andesitic-basaltic lava breccia and lava flows (E_1^{b}), rhyolitic tuff and lava flows (E_1^{r}), dacitic to andesitic lava flows and rhyodacitic pyroclastic (E_1^{da}), bituminous siltstone and shale, calcareous tuffite (E_1^{ss}), tuffaceous sandstone, green tuff (E_1^{st}), shales and siltstone (E_1^{sl}), and green tuffs and limestone (E_1^{tl}). Meanwhile, based on Geology Survey of Iran (GSI 1997), 27.54 % of lithology of study area included by group 4 (Table 1).

Landslides are very common phenomenon in the North of Tehran due to its climate condition. Most of these landslides occur near the rivers and valleys. Velenjak region is located in the North-West of Tehran is one of most sensitive areas. Some other of prone regions are including Ozgol, Dar Abad, North of Saadat Abad, North of Emam Zadeh Ghasem, Oushan-Fasham road, Meygoon, North of Lavasan, North of Kan, and Golab Darreh. Population density and high price of lands of these areas are the main reasons for landslide susceptibility mapping, which can be used for optimum management and also avoidance of susceptible regions.

The most important trusts and faults of study area include of Mosha-Fasham, Purkan-Vardij, North of Tehran trusts, Shirpala and Emamzadeh Davud faults (GSI 1997). The

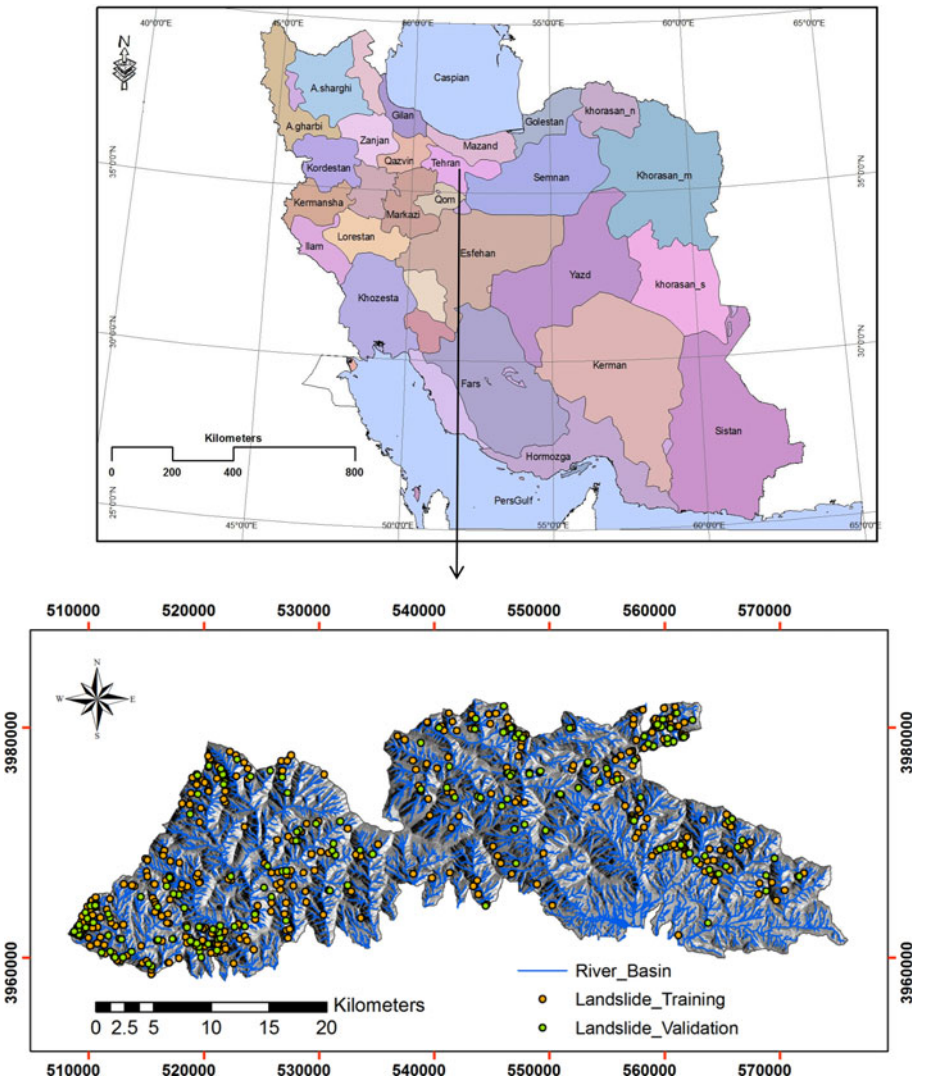

Fig. 1 Landslide location map of study area

altitude of the area ranges from 1,349.5 to 3,952.9 a.m.s.l. The slope angles of the area range from 0° to as much as 83°. The major land use of the study area consists of rangeland and covers almost 90.5 % of the whole area.

3 Conditioning factors database

For any kind of landslide study, a correct landslide database is the pre-requisite (Varnes 1984). Besides, landslide inventory mapping is the most fundamental step in any landslide susceptibility and hazard modeling (Ercanoglu and Gokceoglu 2004). It allows us to

Table 1 Lithology of the study area (GSI 1997)

Code	Group	Formation	Lithology	Geological age
Q^2	1	Sub recent Tehran alluvium-unit C	Young alluvia fans and terraces	Quaternary
Q^l		Kahrizak-unit B	Old alluvial fans and terraces	Quaternary
Q^s		–	Young and old scree, talus deposits	Quaternary
Q^f		–	Young and old alluvial fans, agglomerate	Quaternary
Q_U		–	Undifferentiated young and old alluvial fans and terraces, alluvium, residual soils	Quaternary
Q^{al}		–	Loose alluvium (including recent alluvium-unite D)	Quaternary
Q		–	Conglomeratic terraces and fans	Quaternary
Q^m		–	Morain	Quaternary
Q^{sc}		–	Scree	Quaternary
Q_2^t		–	Young terraces	Quaternary
Q_1^t		–	Old terraces	Quaternary
Q^{tr}	2	–	Spongy porous travertine	Quaternary
PlQ^{sc}	3	Hezardarreh-unit A	Conglomerate, sandstone, mudstone intercalations	Pleistocene
M		Upper red	Undivided Miocene deposits including sandy marl, siltstone, conglomerate, gypsum, Miliolidus limestone	Miocene
M_u^2		Upper red	Sandstone, silty marl, mudstone, siltstone	Miocene
E_{Kn}		Kond	Sandstone, conglomerate, gypsum, Nummuliti marly limestone	Eocene
E_4^{sc}		–	Sandstone, conglomerate, green tuff	Eocene
E_4^{st}		Turbiditic sediments	Light color sandstone, greenish tuffite, conglomerate	Eocene
E_3^{sc}		–	Tuffaceous sandstone, micro-conglomerate with intercalations of tuffite	Eocene
E_3^{tc}		Turbiditic sediments	Tuffite sandstone, conglomerate	Eocene
E_3^{sh}		–	Shale with intercalations of tuffaceous sandstone and siltstone	Eocene
E_f^{sl}		–	Red conglomerate and sandstone with intercalations of limestone	Eocene
E_f^c		–	Red conglomerate, sandstone, and shale	Eocene
E_f^{st}		–	Shale, sandstone, and tuffite with intercalations of limestone	Eocene
E_m		Mila	Medium-thin-bedded limestone with intercalations of shales	Eocene

Table 1 continued

Code	Group	Formation	Lithology	Geological age
E_z		Zagun	Red, green micaceous shales and sandstones	Eocene
PE_z		Ziarat	Alveolina-Nummuliti limestone, conglomerate, gypsum	Paleocene
E_K^m	4	Karaj	Light green-gray laminated calcareous mudstone, shale, tuff, gypsum, tuffite	Eocene
E_K^t		Karaj	Green thick-bedded tuff, tuffaceous shale, minor lava, pyroclastic, tuff, breccia (mainly consisting mid. Tuff member)	Eocene
E_K^{sh}		Karaj	Calcareous and siliceous dark color shale, tuffite, pyroclastic	Eocene
E^{dg}		–	Micro-dioritic-micro-gabbro as sill and dikes	Post-lower Eocene
E_5^{sh}		–	Shale with intercalations of tuffite and tuffaceous sandstone	Eocene
E_5^{tb}		–	Green tuff, tuff breccia, tuffite with intercalations of tuffaceous siltstone	Eocene
E_5^{td}		–	Hyalotrachyandesite, trachte-dacite, tuff breccia	Eocene
E_3^b	5	–	White-green tuff breccia, ash tuff	
E_3^{ss}		–	Alternation of shale and tuffaceous siltstone	Eocene
E_2^t		–	Green crystal, lithic and ash tuff, tuff breccia, and partly with intercalations of limestone	Eocene
E_2^{ts}		–	Alternation of shale and tuffaceous siltstone	Eocene
E_2^r		–	Rhyolitic tuff with some intercalations of shale	Eocene
E_1^{tsv}		–	Massive green tuff, shale with dacitic and andesitic-basaltic lava flows	Eocene
E_1^{sht}		–	Dark gray shale with alternation of green tuff, and partly with sandstone, shale, conglomerate and limestone	Eocene
E_1^{tsh}		–	Alternation of green tuff and shale	Eocene
E_1^b		–	Andesitic-basaltic lava breccia and lava flows	Eocene
E_1^r		–	Rhyolitic tuff and lava flows	Eocene
E_1^{da}		–	Dacitic to andesitic lava flows and rhyodacitic pyroclastic	Eocene
E_1^{ss}		–	Bituminous siltstone and shale, calcareous tuffite	Eocene
E_1^{st}		–	Tuffaceous sandstone, green tuff	Eocene
E_1^{sl}		–	Shales and siltstone	Eocene

Table 1 continued

Code	Group	Formation	Lithology	Geological age
E_l^{tl}		–	Green tuffs and limestone	Eocene
Gy	6	–	Gypsum	Paleocene
$PE_f^{m,s,c}$		Fajan	Marl, sandstone, conglomerate, gypsum	Paleocene
PE_f^{c}		Fajan	Thick-bedded to massive polygenetic conglomerate, sandstone, locally limestone beds	Paleocene
PE^{v}		–	Andesitic-dacitic rocks, red–purple agglomerate, pyroclastic, tuffs	Paleocene
K_u^{b}	7	–	Thin-bedded limestone	Turonian-Early Senonian
J_l		Lar	Thin-bedded to massive limestone, in some plates may include undivided Dalihai formation	Jurassic
J_d		Dalihai	Thin-bedded marly limestone, marl, Ammonite bearing	Jurassic
TR_3J_s		Shemshak	Shale, sandstone, siltstone, clay stone, locally limestone intercalations, coal bearing	Triassic
TR_e^{d}		Elika	Thick-bedded massive dolomites and dolomitic limestone	Triassic
TR_e^{l}		Elika	Thick-bedded to massive limestone	Triassic
$TR_e^{m,l}$		Elika	Platy marly limestone, Oolitic limestone	Triassic
P_n		Nesen	Marly limestone	Triassic
P_r		Ruteh	Medium-bedded limestone	Permian
C		Mobarak limestone	Dark gray medium-bedded limestone with intercalations of marly limestone	Carbonifer
C_j^{c}		Jeirud	Light gray massive dolomitic limestone	Carbonifer
C_j^{b}		Jeirud	Black limestone, clayey marl intercalations	Carbonifer
C_j^{d}		Jeirud	Black Oolitic and intraclastic limestone	Carbonifer
m		Mobarak	Black Oolitic, dolomitic limestone, marl intercalations	Miocene
D_j^{a}		Jeirud	Sandstone, shale, limestone, marl, phosphatic layers	Devonian
E_m		Mila	Trilobite-bearing limestone, marl, dolomite, and shale	Eocene
E^{q}	8	–	White quartzite, quartzitic sandstone (formly top quartzite)	Eocene
E_l		Lalun	Red arkosi sandstone	Eocene
E_{bt}		Barut	Miaeous variegated siltstone and shale, cherty dolomite intercalations	Eocene

Table 1 continued

Code	Group	Formation	Lithology	Geological age
E^{d}_{bt}		Barut	Black massive dolomite, green-black shale intercalations	Eocene
T^{b}		–	Basic and intermediate sills	Tertiary, mostly Oligocene
T^{s}		–	Mostly syenite and some leuosyenite porphyry	Tertiary, mostly Oligocene
E^{d}		–	Dacitic dikes	Lower Eocene
E^{s}_{6}		–	Gray-brown shale, siltstone, and sandstone	Eocene

develop knowledge about the past landslide types, failure mechanisms, and conceptual knowledge about relations between existing landslide and conditioning and triggering factors (Ghosh 2011). Inventories are prepared using different techniques depending on the scope of the work, the extent of the study area, the scales of base maps, the quality and detail of the accessible information, and the resources available to carry out the work (Guzzetti et al. 2000). In the study area, a total of 528 landslides were mapped at 1:25,000-scale, using aerial photograph, satellite images, and field survey. Some views of the recent landslides identified in the study area are shown in Fig. 2. The smallest landslide that was mapped form above source and recognized in the field had an extent of 685 m^2, while the largest was 280,804 m^2. The modes of failure for the landslides identified in the study area were determined according to the landslide classification system proposed by Varnes (1978). Most of the landslides are shallow rotational with a few translational. However, during the analyses performed in the present study, only rotational failure is considered and translational slides were eliminated because its occurrence is rare. In this research, the landslide inventory was randomly split into a testing dataset 70 % (370 landslide locations) for training the adopted models and the remaining 30 % (158 landslides locations) was used for validation purpose (Fig. 1). Identification of a suitable set of instability factors bearing a relationship with slope failures requires an a priori knowledge of the main causes of landslides (Guzzetti et al. 1999).

In order to landslide susceptibility zoning of the study area, twelve landslide conditioning factors were considered. These factors are slope degree, slope aspect, altitude, plan curvature, normalized difference vegetation index, land use, lithology, distance from rivers, distance from roads, distance from faults, stream power index (SPI), and slope-length (LS) (Table 2).

A digital elevation model (DEM) was created from 13 adjacent topographic sheets (digitalization of contours at a 10 m interval and points) at 1:25,000-sclae. The DEM map has a grid size of 10 m with 2,452 rows and 6,768 columns. The digital elevation model has been subsequently used to derive the slope degree, slope aspect, altitude, and plan curvature, which are considered as important topographic factors for stability of the terrain. The slope map of the study area is derived from the DEM using the slope function in ILWIS-GIS. These slope values (in degree) are divided into five different classes are (1) flat-gentle slope <5°, (2) fair slope (5–15°), (3) moderate slope (15–30°), (4) steep slope (30–50°), and (5) very steep slope >50° (Fig. 3a). Slope aspect strongly affects hydrologic

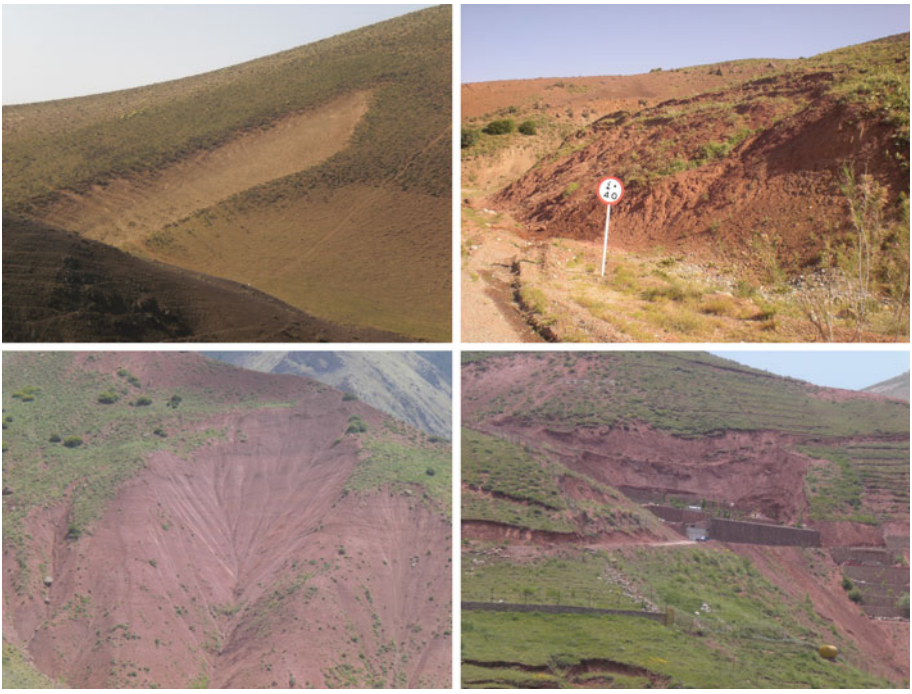

Fig. 2 Field photographs of some occurred landslides in study area

Table 2 Landslide database of study area

Data layers	GIS data type	Scale
Landslide inventory map	Polygon coverage	1:25,000
Topographic map	Line and point coverage	1:25,000
Geology map	Polygon and line coverage	1:100,000
Land use map	Polygon coverage	LISS-III (23.5 m × 23.5 m) and Pan (2.5 m × 2.5 m)
NDVI	GRID	LISS-III (23.5 m × 23.5 m) and Pan (2.5 m × 2.5 m)

processes via evapo-transpiration, direction of frontal precipitation, and thus affects weathering processes and vegetation and root development, especially in drier environments (Sidle and Ochiai 2006). Aspect layer has been categorized into nine classes (Fig. 3b): (1) Flat, (2) north, (3) northeast, (4) east, (5) southeast, (6) south, (7) southwest, (8) west, and (8) northwest. The altitude does not contribute directly to landslide manifestation, but in relation to the other parameters, like tectonics, erosion–weathering processes, and precipitation, the altitude contributes to landslide manifestation and influences the whole system (Rozos et al. 2008). The altitude map for study area with cell size 10 × 10 m was produced from the DEM and classified into 6 classes, that is, (1)

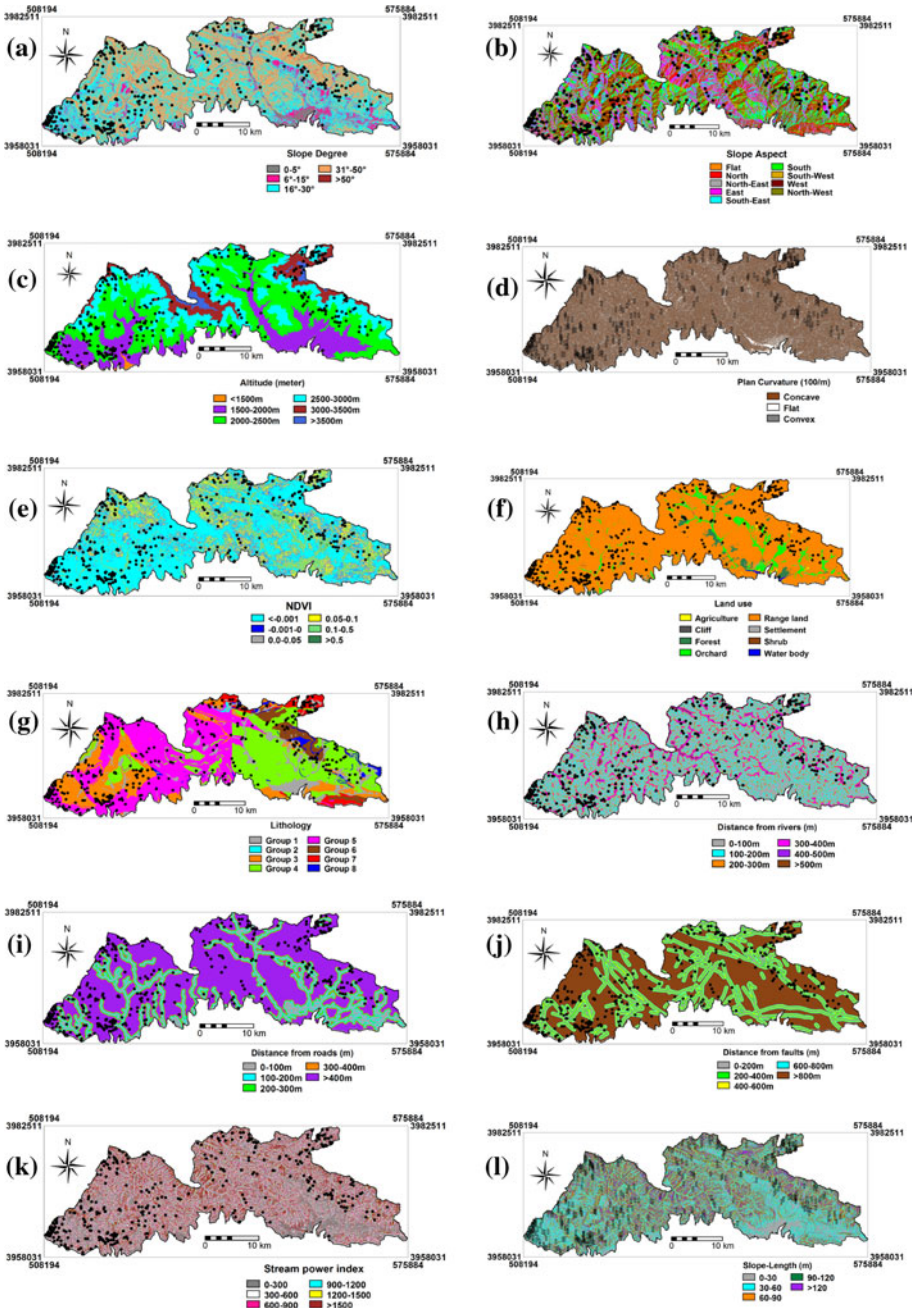

Fig. 3 Landslide conditioning factors of the study area; **a** slope degree, **b** slope aspect, **c** altitude, **d** plan curvature, **e** NDVI, **f** land use; **g** lithology; **h** distance from rivers; **i** distance from roads; **j** distance from faults; **k** SPI; **l** slope-length

<1,500 m, (2) 1,500–2,000 m, (3) 2,000–2,500 m, (4) 2,500–3,000 m, (5) 3,000–3,500 m, and (6) >3,500 m (Fig. 3c). The curvature represents the morphology of the topography. A positive curvature indicates that the surface is upwardly convex at that cell, and a negative curvature indicates that the surface is upwardly concave at that cell. A value of zero indicates that the surface is flat (Oh and Lee 2010) (Fig. 3d). The normalized difference vegetation index is a measure of surface reflectance and gives a quantitative estimate of the vegetation growth and biomass (Hall et al. 1995; Yilmaz 2009). Using the satellite images of Indian remote sensing (IRS) by sensors LISS-III and panchromatic, the NDVI was taken into consideration as a landslide-related factor (Fig. 3e). The NDVI was calculated from the following equation:

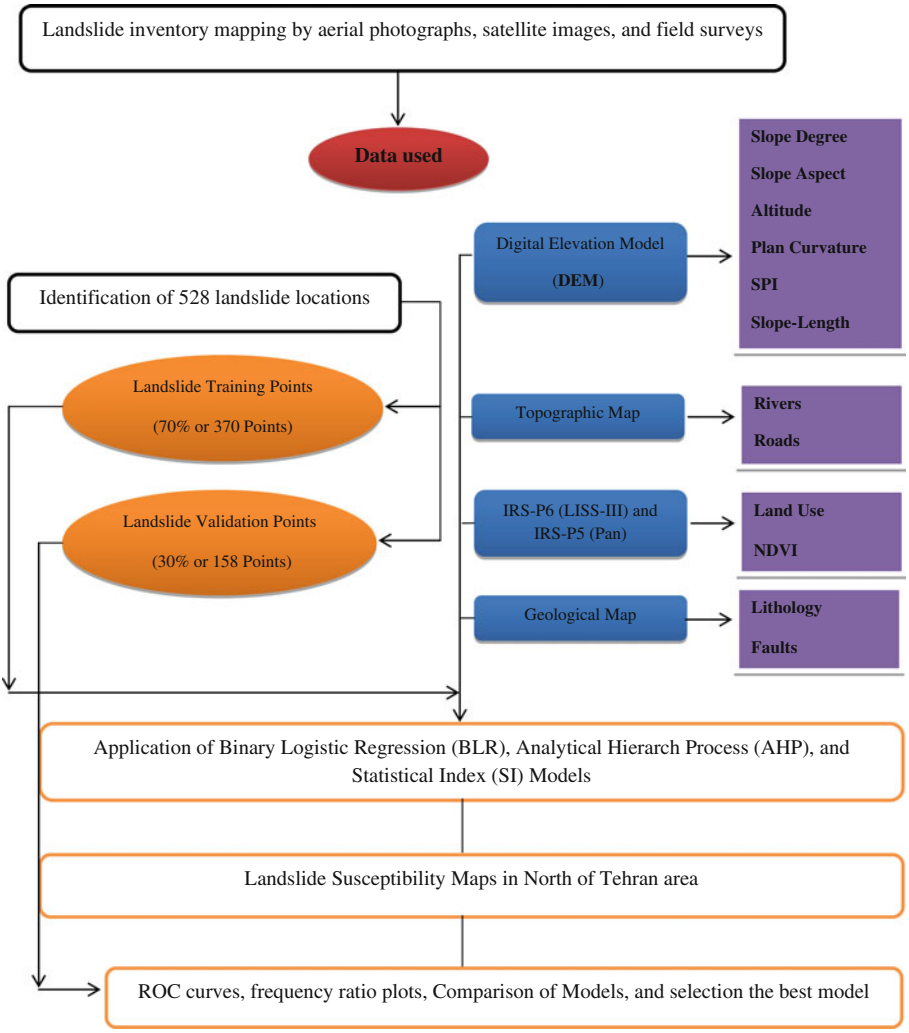

Fig. 4 Flowchart of methodology

$$\mathrm{NDVI} = \{(\mathrm{IR} - \mathrm{R})/(\mathrm{IR} + \mathrm{R})\} \quad (1)$$

where, IR, infrared portion of the electromagnetic spectrum; R, red portion of the electromagnetic spectrum.

Land use layer was prepared using IRS-LISS-III and panchromatic remote sensing images. The supervised classification and maximum likelihood algorithm is assigned in order to create this map. The area is covered by eight land use types that are agricultural land, cliff, forest, orchard, range land, settlement area, shrubs, and water body. The details of land use type are shown in Fig. 3f and summarized in Table 7. The study area is covered dominantly by range land area (90.51 %). Lithological features are represented in the geological map of the study area (Fig. 3g), which is derived from the two geological maps of Tehran and east of Tehran in scale of 1:100,000. The mentioned map was prepared by geological survey of Iran (1997), digitized in ILWIS-GIS (integrated land and water information system), and divided into eight groups (Table 1). The drainage system of any area plays an important role in slope stability particularly with respect to toe cutting and bank erosion (Miller and Sias 1998). The distance from rivers was calculated using the vector river lines by applying the distance function available in the ArcGIS. Six classes corresponding to distance from river were calculated at 100-m intervals (Fig. 3h). In mountainous region, any disturbance on natural slopes, such as road cutting, may cause the initiation of mass movements (Nefeslioglu et al. 2008). Accordingly, these types of territories, it could be helpful to consider the proximity of roads as a conditioning parameter in landslide occurrence. The map of distance from roads was also constructed by buffering having the respective intervals of 100 m (Fig. 3i). The distance from faults was extracted from the structural geology map of study area at 1:100,000-scale. Five buffers at 200-m class interval around faults were created. The fault buffer categories were thus defined as (1) 0–200 m, (2) 200–400 m, (3) 400–600 m, (4) 600–800 m, and (5) >800 m (Fig. 3j). In this study, two well-known secondary geo-morphometric factors were also evaluated. These factors are stream power index and slope-length (Fig. 3k, l). These conditioning factors were derived based on slope map and specific catchment area (A_S) (Moore and Burch 1986; Moore et al. 1991).

$$\mathrm{SPI} = (\tan\beta \times A_S) \quad (2)$$

$$\mathrm{LS} = \left(A_S/22.13\right)^{0.6} \times \left(\sin\beta/0.0896\right)^{1.3} \quad (3)$$

where β is the slope angle in degree and A_S is calculated based on following equation (Hengl et al. 2003):

$$A_S = \left(A_m \times P^2 \Big/ \sum L_i\right) \quad (4)$$

In the above equation, P is the pixel size, A_m is the cumulative drainage fraction from m neighbors, and $\sum L_i$ is derived as the sum of lengths for drainage pixels.

Stream power index is a measure of the erosive power of flowing water based on the assumption that discharge is proportional to specific catchment area. Also, the slope-length (LS) factor in the Universal Soil Loss Equation (Eq. 3) is a measure of the sediment transport capacity of overland flow (Moore and Wilson 1992).

Table 3 The fundamental scale of absolute numbers (Saaty 2008)

Intensity of importance	Definition	Explanation
1	Equal importance	Two activities contribute equally to the objective
2	Weak or slight	
3	Moderate importance	Experience and judgement slightly favor one activity over another
4	Moderate plus	
5	Strong importance	Experience and judgement strongly favor one activity over another
6	Strong plus	
7	Very strong or demonstrated importance	An activity is favored very strongly over another; its dominance demonstrated in practice
8	Very, very strong	
9	Extreme importance	The evidence favoring one activity over another is of the highest possible order of affirmation
Reciprocals of above	If activity I has one of the above nonzero numbers assigned to it when compared with activity j, then j has the reciprocal value when compared with i	A reasonable assumption
1.1–1.9	If the activities are very close	May be difficult to assign the best value but when compared with other contrasting activities
		The size of the small numbers would not be too noticeable, yet they can still indicate the relative importance of the activities

4 Methodology

As mentioned previously, the main purpose of the present study is to investigate and comparison of the landslide susceptibility mapping using three models such as binary logistic regression, analytical hierarchy process, and statistical index in the north of Tehran metropolitan, Iran. Figure 4 shows the landslide susceptibility analysis and methodology flowchart used in this study.

4.1 Binary logistic regression (BLR)

The binary logistic model, as a nonlinear regression model, is a special case of a generalized linear model (Schumacher et al. 1996). The goal of logistic regression is to find the best model to describe the relationship between a dependent variable and multiple independent variables (Ohlmacher and Davis 2003; Lee 2005; Ozdemir 2011). The advantage of logistic regression is that, through the addition of an appropriate link function to the usual linear regression model, the variables may be either continuous or discrete, or any combination of both types and they do not necessarily have normal distributions (Lee and Pradhan 2007). The algorithm of logistic regression applies maximum likelihood estimation after transforming the dependent variable into a logic variable representing the natural

Table 4 Beta coefficients and test statistics of the variables used in the logistic regression equation

Conditioning factors	*B*	SE	Wald	*df*	Significance	Exp (*B*)
Slope degree	−2.643	1.457	3.291	1	.070	.071
Aspect (Flat)	11.657	1,051.286	.000	1	.991	115,540.320
Aspect (North)	16.336	1,051.289	.000	1	.988	1.244E7
Aspect (Northeast)	.470	1,569.861	.000	1	1.000	1.600
Aspect (East)	1.547	1,355.837	.000	1	.999	4.698
Aspect (Southeast)	3.448	1,248.227	.000	1	.998	31.443
Aspect (South)	17.566	1,051.299	.000	1	.987	4.252E7
Aspect (Southwest)	−3.174	1,467.256	.000	1	.998	.042
Altitude	−.023	.013	2.822	1	.093	.978
Plan curvature	−11.197	110.365	.010	1	.919	.000
NDVI	1.930	13.996	.019	1	.890	6.888
Land use (range land)	.875	3,353.479	.000	1	1.000	2.398
Lithology (Group 1)	2.473	5,128.669	.000	1	1.000	11.858
Lithology (Group 2)	−8.171	976.674	.000	1	.993	.000
Lithology (Group 3)	13.738	872.773	.000	1	.987	925,652.247
Lithology (Group 4)	−4.795	2,471.153	.000	1	.998	.008
Distance from rivers	.042	.027	2.380	1	.123	1.043
Distance from roads	.009	.006	1.974	1	.160	1.009
Distance from faults	.030	.017	3.063	1	.080	1.031
SPI	−.050	.031	2.629	1	.105	.951
Slope-length	1.524	.902	2.855	1	.091	4.593
Constant	−.016	3,621.269	.000	1	1.000	.985

logarithm of the odds of the dependent occurring or not (Atkinson and Massari 1998; Bai et al. 2010). The mentioned model can be expressed according to following equation (Lee and Pradhan 2007):

$$P = \left(\frac{1}{1 + e^{-Z}}\right) \tag{5}$$

where, P is the estimated probability of landslide occurrence and varies from 0 to 1 on and S-shaped curve, and Z is the linear combination while defined as the following Equation (Eq. 6) and its value varies from $-\infty$ to $+\infty$:

$$Z = \text{intercept} + b_1x_{1+}b_2x_{2+}b_3x_{3+}\ldots b_nx_n \tag{6}$$

where b_1, b_2, b_3, and b_n, are the slope coefficient of the logistic regression model and x_1, x_2, x_3, and x_n are the independent variables.

4.2 Analytical hierarchy process (AHP)

The analytical hierarchy process is a theory of measurement for considering tangible and intangible criteria that has been applied to numerous areas, such as decision theory and conflict resolution (Vargas 1990; Yalcin 2008). The AHP is an eigenvalue technique to the pair-wise comparisons approach. It is based on three principles: decomposition,

Table 5 The multi-collinearity diagnosis indexes for variables

Model	Unstandardized coefficients		Standardized coefficients	*t*	Sig.	Collinearity statistics	
	B	SE	Beta			Tolerance	VIF
(Constant)	.006	.009		.665	.506		
Slope degree	−9.460E−5	.000	−.027	−1.466	.143	.874	1.144
Slope aspect	.000	.000	−.008	−.458	.647	.847	1.181
Altitude	−1.834E−6	.000	−.015	−.806	.420	.829	1.207
Plan curvature	−.005	.039	−.002	−.123	.902	.753	1.327
NDVI	−9.889E−5	.007	.000	−.014	.989	.875	1.142
Land use	.000	.001	.002	.130	.896	.928	1.078
Lithology	.000	.000	.015	.835	.404	.897	1.115
Distance from rivers	4.774E−6	.000	.019	1.108	.268	.970	1.031
Distance from roads	1.707E−7	.000	.004	.209	.834	.802	1.247
Distance from faults	3.783E−6	.000	.042	2.306	.021	.850	1.177
SPI	−5.861E−9	.000	−.010	−.462	.644	.601	1.663
Slope-length (LS)	−2.377E−6	.000	−.006	−.249	.803	.496	2.018

comparative judgment, and synthesis of priorities (Saaty 1994; Chen et al. 2009). The decomposition principle is applied to structure a complex problem into a hierarchy of clusters, sub-clusters, and so on (Kheirkhah Zarkesh 2005). The comparative judgment principle of AHP requires pair-wise comparison of the decomposed elements within a given level of hierarchal structure with respect to the next higher level. The synthesis principle of AHP takes each of the derived ratio scale local priorities in the various levels of the hierarchy and constructs a composite set of priorities for the elements at the lowest level of the hierarchy (Chen et al. 2009). The AHP provides a numerical fundamental scale, which ranges from 1 to 9 to calibrate the quantitative and qualitative performances of priorities (Table 3) (Saaty 2008). This matrix ultimately enters in expert choice (EC) software and will calculate final weight for each conditioning factor with consistency ratio (CR). If CR is less than 10 %, then the matrix can be considered as having an acceptable consistency (Saaty 1977). Finally, the landslide susceptibility map using AHP model was constructed using the following equation:

$$\begin{aligned} \mathrm{LSM_{AHP}} = {} & ((\text{slope degree} \times W_{\mathrm{AHP}}) + (\text{slope aspect} \times W_{\mathrm{AHP}}) + (\text{altitude} \times W_{\mathrm{AHP}}) \\ & + (\text{plan curvature} \times W_{\mathrm{AHP}}) + (\text{NDVI} \times W_{\mathrm{AHP}}) + (\text{land use} \times W_{\mathrm{AHP}}) \\ & + (\text{lithology} \times W_{\mathrm{AHP}}) + (\text{distance from rivers} \times W_{\mathrm{AHP}}) \\ & + (\text{distance from roads} \times W_{\mathrm{AHP}}) \\ & + (\text{distance from faults} \times W_{\mathrm{AHP}}) + (\text{SPI} \times W_{\mathrm{AHP}}) + (\text{LS} \times W_{\mathrm{AHP}})) \end{aligned} \quad (7)$$

where W_{AHP} is the weightage for the each landslide conditioning factor.

4.3 Statistical index (SI)

The statistical index method is a bivariate statistical analysis proposed by van Westen (1997) for landslide susceptibility mapping. A weight value for each categorical unit is defined as the natural logarithm of the landslide density in the categorical unit divided by the landslide

Table 6 The weight each conditioning factors by analytical hierarchy process

Conditioning factors	(1)	(2)	(3)	(4)	(5)	(6)	(7)	(8)	(9)	(10)	(11)	(12)	Weight
(1) Slope degree	1	3	3	2	2	2	1/2	3	3	3	4	4	0.15
(2) Slope aspect		1	2	1/3	1/2	1/2	1/4	2	3	2	3	3	0.07
(3) Altitude			1	1/3	1/2	1/2	1/4	3	2	3	2	2	0.06
(4) Plan curvature				1	3	2	1/2	2	2	3	4	4	0.13
(5) DVI					1	1	1/3	2	2	3	3	3	0.08
(6) Land use						1	1/2	4	3	4	5	4	0.11
(7) Lithology							1	5	4	4	6	6	0.21
(8) Distance from rivers								1	1/2	2	2	4	0.05
(9) Distance from roads									1	3	4	3	0.06
(10) Distance from faults										1	3	3	0.04
(11) SPI											1	4	0.03
(12) LS												1	0.02
Inconsistency ratio = 0.0676													

density in the entire map (van Westen 1997; Rautela and Lakhera 2000; Cevik and Topal 2003). This method is based on the following equation (van Westen 1997):

$$W_{\mathrm{SI}} = \ln\left(\frac{E_{ij}}{E}\right) = \ln\left(\frac{L_{ij}/L_{\mathrm{T}}}{P_{ij}/P_{\mathrm{L}}}\right) \tag{8}$$

where, W_{SI}, weight given to a certain class i of parameter j; E_{ij}, landslide density within class i of parameter j; E, total landslide density within the entire map; L_{ij}, number of landslides in a certain class i of parameter j; P_{ij}, number of pixels in a certain class i of parameter j; L_{T}, total number of landslides in the entire map; P_{L}, total pixels of the entire map.

Yesilnacar (2005) is stated that the bivariate statistical method gives a satisfactory combination of the (subjective) professional direct mapping and the (objective) data driven analytical capabilities of a GIS. The main advantage of bivariate statistical procedures is that the professional, who executes the analysis, determines the factors or combinations of factors used in the assessment.

In the current research, every parameter map is crossed with the landslide inventory map, and the density of the landslide in each class is calculated. The statistical index map is created by the overlay method in ArcGIS. Positive values of W_{SI} indicate a relevant relationship between the presence of the factor class and landslide distribution, the stronger the higher the score. In contrary, negative values of W_{SI} mean that the presence of the factor class is not relevant in landslide development.

5 Results

5.1 Binary logistic regression

The binary logistic regression analysis was performed using the statistical package for the social sciences (SPSS). In order to process the input data layers, all the conditioning factors and landslides were converted into grid format and then into ACSII data format (Devkota et al. 2013). ASCII data of each map were exported to SPSS, and then the binary logistic

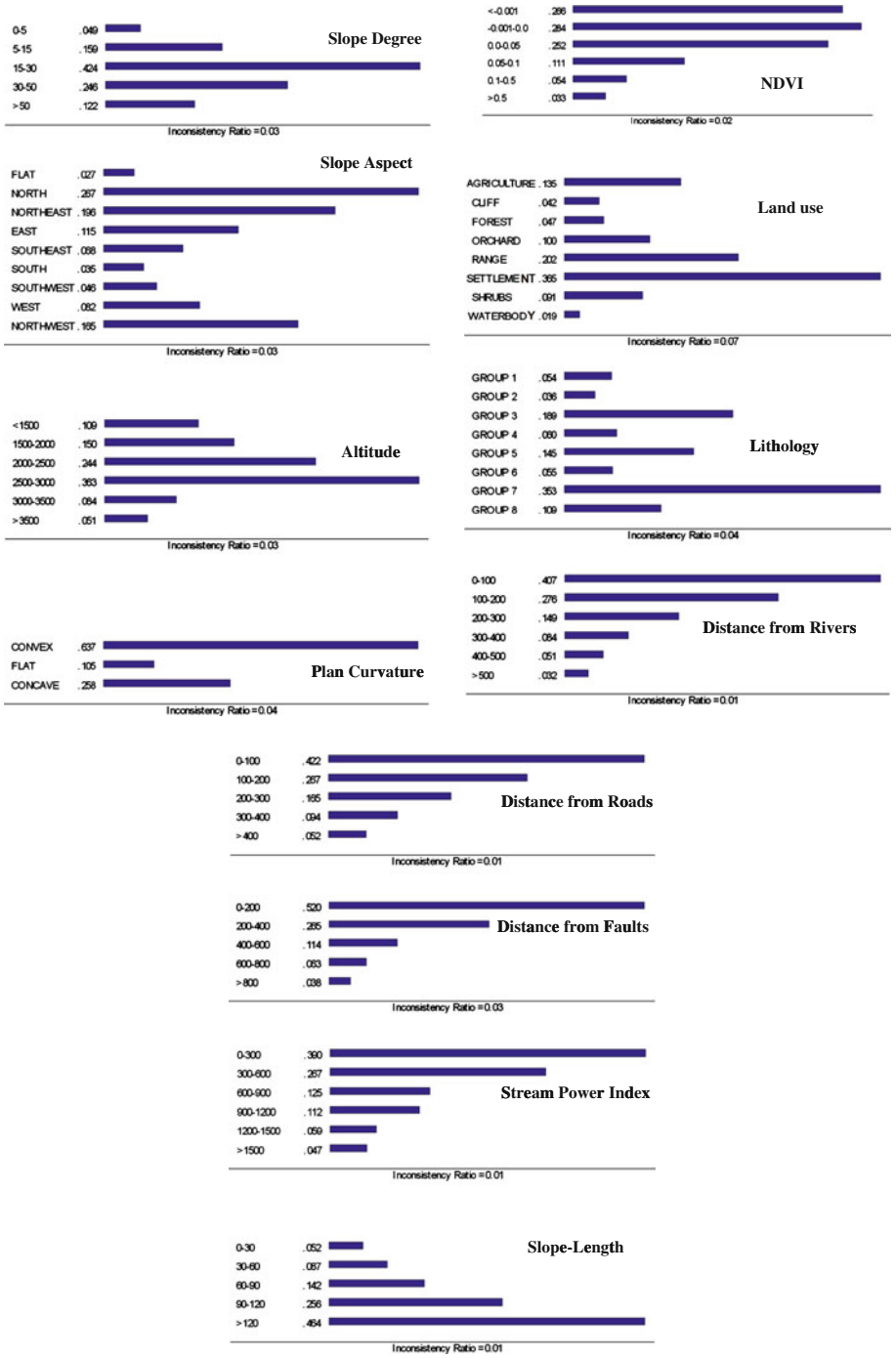

Fig. 5 Results of AHP for sub-objectives of conditioning factors in expert choice (EC) software

regression model was run to obtain the coefficients of the landslide conditioning factors for numerical and categorical data. The Hosmer and Lemeshow test showed that the goodness of fit of the equation can be accepted, because the significance of chi-square is larger than 0.05 (1.00). The value of Cox and Snell R^2 (0.009) and Nagelkerke R^2 (0.624) showed that the independent variables can explain the dependent variables in a way.

The β coefficient of each conditioning factor is shown in Table 4. According to Table 4, it is observed that normalized different vegetation index (NDVI), slope-length (LS), distance from rivers, distance from faults, and distance from rivers have an important role in the landslide susceptibility mapping of study area, because of positive β value. The β values of these conditioning factors are 1.930, 1.524, 0.042, 0.030, and 0.009, respectively. On the other hand, slope degree, altitude, and stream power index (SPI) have negative effect in landslide occurrence with β values of -2.643, -0.023, and -0.050, respectively. In the case of slope aspect, south ($\beta = 17.566$), north ($\beta = 16.336$), flat ($\beta = 11.656$), southeast ($\beta = 3.448$), east ($\beta = 1.547$), and northeast ($\beta = 0.470$) facing have positive β coefficient. In the contrary, southwest facing has value of -3.174. For land use factor, results showed that only range land type has an effect on landslide susceptibility with value of 0.875, while the remaining land use types does not have any role in landslide occurrence of the north of Tehran. Based on results of logistic regression for lithology factor, we seen that lithological formation of groups 3 and 1 (Table 1) have positive β value, whereas groups of 2 and 4 with negative value of -8.171 and -4.795 have an inverse effect on landslide susceptibility.

5.2 Multi-collinearity in binary logistic regression

An important consideration in regression is the effect of correlation among independent variables. There is a problem that exists when two independent variables are very highly correlated. The problem is called multi-collinearity. Tolerance and the variance inflation factor (VIF) are two important indexes for multi-collinearity diagnosis. In fact, tolerance is $1-R^2$ for the regression of that variable against all the other independents, without the dependent variable. On the other hand, VIF is simply the reciprocal of tolerance. VIF measures the degree to which the interrelatedness of the variable with other predictor variables inflates the variance of the estimated regression coefficient for the variable. Consequently, the square root of the VIF is the degree to which the collinearity has increased the standard error for that variable. A tolerance of less than 0.20 or 0.10 and/or a VIF of 5 or 10 and above indicates a multi-collinearity problem (O'Brien 2007). According to Table 5, the smallest tolerance and highest variance inflation factor were 0.496 and 2.018, respectively. So, there is not any multi-collinearity between independent factors in current research. Finally, the BLR model developed for the study area is given in Eq. 9.

$$\begin{aligned} Z = \{&-0.016 + (\text{slope degree} \times -2.643) + (\text{slope aspect}) + (\text{altitude} \times -0.023) \\ &+ (\text{plan curvature} \times -11.197) + (\text{NDVI} \times 1.930) + (\text{land use}) + (\text{lithology}) \\ &+ (\text{distance from rivers} \times 0.042) + (\text{distance from roads} \times 0.009) \\ &+ (\text{distance from faults} \times 0.030) + (\text{SPI} \times -0.050) + (\text{LS} \times 1.524)\} \end{aligned} \tag{9}$$

5.3 Analytical hierarchy process (AHP)

AHP is a multi-objective, multi-criteria decision-making approach, which enables the user to arrive at a scale of preference drawn from a set of alternatives (Saaty 1980). The expert choice software package (E.C. Inc. 1995) based on the analytic hierarchy process (AHP)

Table 7 Spatial relationship between each landslide conditioning factors and landslide by statistical index model

Factor	Class	No. of pixels in domain P_{ij}	No. of landslide (L_{ij})	Statistical index (SI)
Slope degree	0–5°	208,056	1	−2.15
	5–15°	810,093	9	−1.31
	15–30°	3,821,708	194	0.21
	30°–50°	4,084,952	165	−0.02
	>50°	64,615	1	−0.98
Slope aspect	Flat	2,311	0	None
	North	746,415	39	0.24
	Northeast	925,769	72	0.64
	East	1,164,311	63	0.27
	Southeast	1,261,381	43	−0.19
	South	1,410,918	39	−0.40
	Southwest	1,488,757	46	−0.29
	West	1,139,281	33	−0.35
	Northwest	850,281	35	8.22E−05
Altitude (m)	<1,500	28,167	1	−0.15
	1,500–2,000	1,794,843	49	−0.41
	2,000–2,500	3,742,774	164	0.06
	2,500–3,000	2,386,544	112	0.13
	3,000–3,500	878,385	40	0.10
	>3,500	158,711	4	−0.49
Plan curvature (100/m)	Concave	3,730,908	154	0.003
	Flat	768,185	25	−0.23
	Convex	4,490,331	191	0.03
NDVI	<−0.001	5,104,044	234	0.11
	−0.001–0.00	389,157	12	−0.29
	0.0–0.05	1,579,113	62	−0.05
	0.05–0.1	835,563	39	0.13
	0.1–0.5	1,060,265	23	−0.64
	>0.5	21,282	0	None
Land use	Agriculture	12,673	0	None
	Cliff	9,643	0	None
	Forest	207,254	4	−0.76
	Orchard	540,179	1	−3.10
	Range land	8,137,410	365	0.09
	Settlement	49,206	0	None
	Shrub	17,666	0	None
	Water body	15,393	0	None

Table 7 continued

Factor	Class	No. of pixels in domain P_{ij}	No. of landslide (L_{ij})	Statistical index (SI)
Lithology	Group 1	919,687	22	−0.54
	Group 2	15,945	0	None
	Group 3	1,597,077	87	0.28
	Group 4	2,474,738	66	−0.43
	Group 5	3,055,530	150	0.18
	Group 6	426,844	7	−0.92
	Group 7	308,607	30	0.86
	Group 8	190,996	8	0.02
Distance from rivers (m)	0–100 m	3,587,993	116	−0.24
	100–200 m	2,612,101	121	0.12
	200–300 m	1,623,562	91	0.31
	300–400 m	819,441	30	−0.12
	400–500 m	276,267	11	−0.03
	>500 m	70,060	1	−1.06
Distance from roads (m)	0–100 m	1,066,777	17	−0.95
	100–200 m	826,979	23	−0.39
	200–300 m	689,664	30	0.06
	300–400 m	622,091	30	0.16
	>400 m	5,783,913	270	0.13
Distance from faults (m)	0–200 m	1,053,403	33	−0.27
	200–400 m	988,251	36	−0.12
	400–600 m	877,027	25	−0.37
	600–800 m	785,670	40	0.21
	>800 m	5,285,073	236	0.08
Stream power index (SPI)	0–300	2,108,573	56	−0.44
	300–600	1,984,601	97	0.17
	600–900	1,288,914	77	0.37
	900–1,200	799,175	36	0.09
	1,200–1,500	512,775	24	0.13
	>1,500	2,295,386	80	−0.17
Slope-length (m)	0–30	1,332,777	25	−0.79
	30–60	2,789,349	134	0.15
	60–90	2,552,783	127	0.19
	90–120	1,147,793	49	0.04
	>120	1,166,722	35	−0.32

Total of pixels in domain (P_T) = 8,989,424; total of landslides (L_T) = 370

has been used to estimate weights of the importance of the major objectives (conditioning factors) and their sub-objectives for landslide susceptibility mapping and to test for consistency ratio (CR) between preferences within individual stakeholder groups. In order to calculate of CR, we used of following equation:

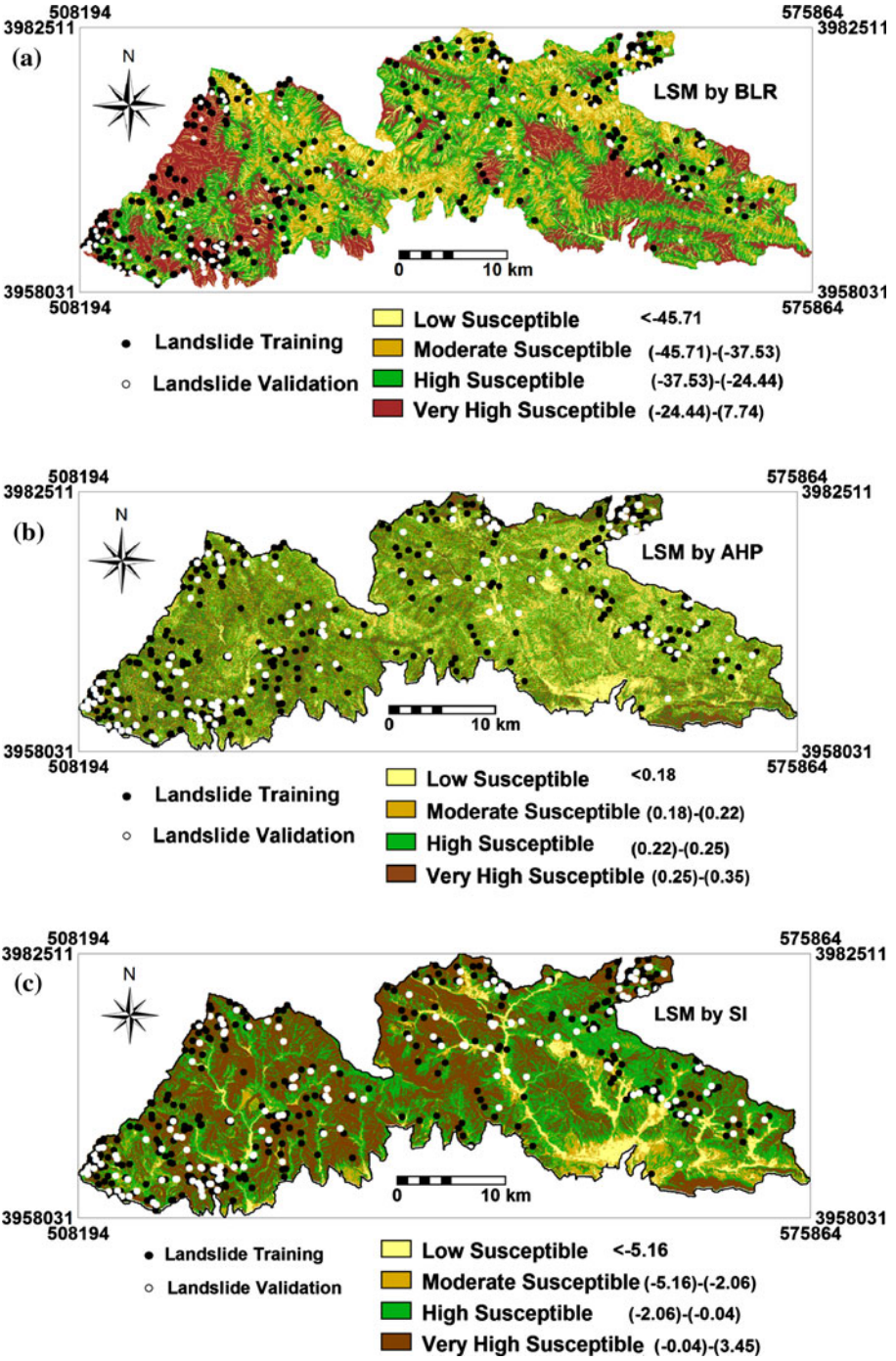

Fig. 6 **a** Landslide susceptibility map based on binary logistic regression (BLR). **b** Landslide susceptibility map based on analytical hierarchy process (AHP). **c** Landslide susceptibility map based on statistical index (SI)

$$\mathrm{CR} = (\mathrm{CI}/\mathrm{RI}) \tag{10}$$

where RI is the average of the resulting consistency index depending on the order of the matrix given by Saaty (1980) and CI is the consistency index and can be expressed as:

$$\mathrm{CI} = ((\lambda_{\max} - n)/(n-1)) \tag{11}$$

where $\lambda_{\max}$ is the largest or principal eigenvalue of the matrix and can be easily calculated from the matrix, and n is the order of the matrix. A CR of 0.1 or less is a reasonable level of consistency (Malczewski 1999). A CR above 0.1 requires revision of the judgment in the matrix due to an inconsistent treatment of particular factor ratings.

Using of AHP method, the levels of the influence of major objectives (conditioning factors) were calculated (Table 6). According to Table 6, it can be seen that lithology and slope-length (LS) factors have the most and less influence on landslide occurrence with values of 0.21 and 0.02, respectively. The other factors such as slope degree, slope aspect, altitude, plan curvature, NDVI, land use, distance from rivers, distance from roads, distance from faults, and SPI have weight values of 0.15, 0.07, 0.06, 0.13, 0.08, 0.11, 0.05, 0.06, 0.04, and 0.03, respectively. In current study, the CR is 0.0676; the ratio indicates a reasonable level of consistency in the pair-wise comparisons.

Also, the correlation between the landslide locations and the sub-objectives of conditioning factors was presented in Fig. 5. The values are given in Fig. 5 show that all CR values are less than 0.1, and consequently, this proves the preferences utilized to produce the comparison matrixes are consistent. In order to landslide susceptibility mapping by analytical hierarchy process, we were used of the following equation:

$$\begin{aligned}\mathrm{LSM_{AHP}} = \{&(\text{slope degree} \times 0.15) + (\text{slope aspect} \times 0.07) + (\text{altitud} \times 0.06)\\ &+ (\text{plan curvature} \times 0.13) + (\text{NDVI} \times 0.08) + (\text{land use} \times 0.11)\\ &+ (\text{lithology} \times 0.21) + (\text{distance from rivers} \times 0.05)\\ &+ (\text{distance from roads} \times 0.06) + (\text{distance from faults} \times 0.04)\\ &+ (\text{SPI} \times 0.03) + (\text{LS} \times 0.02)\}\end{aligned} \tag{12}$$

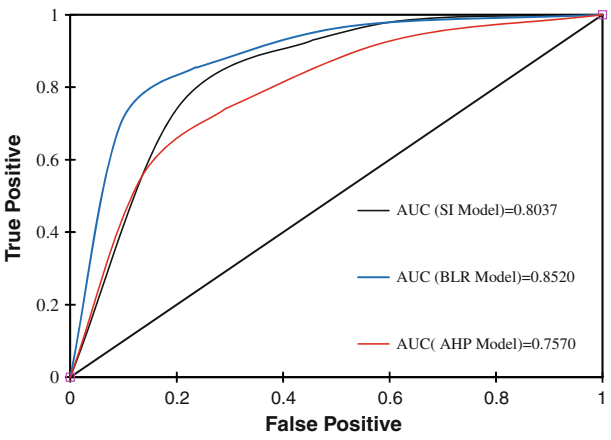

Fig. 7 Comparison of ROC curve (AUC) of landslide susceptibility maps

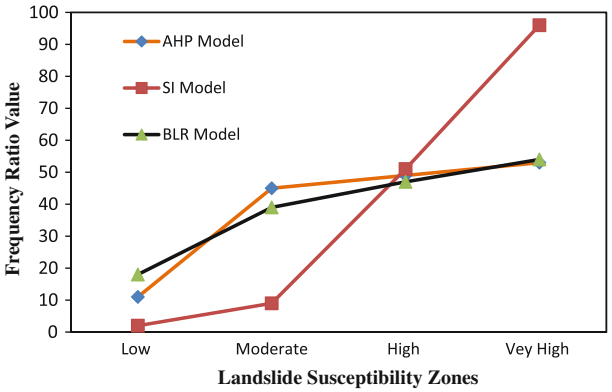

Fig. 8 Frequency ratio plots of four landslide susceptibility zones of landslide susceptibility models

5.4 Statistical index (SI)

Spatial relationship between each landslide conditioning factor and landslide by statistical index model is shown in Table 7. According to Table 7, in the case of slope degree, class of 15°–30° has the highest value of SI with a positive value (0.21), and other classes have negative value. On the other hand, our observation showed that when slope degree is increasing, statistical index is decreasing. For slope aspect conditioning factor, north, northeast, and east facing have a positive value of SI (0.24, 0.64, and 0.27, respectively). This means that the landslide probability is higher in these classes. The statistical index (SI) value for altitude clearly showed that ranges of 2,500–3,000 and 3,000–3,500 m have the most effect on landslide occurrence. However, it is clear that the landslide susceptibility increases by the increase in altitude up to a certain extent (2,500–3,000 m) and then it decreases. In the case of plan curvature, the SI value is positive (0.003 and 0.03) both in concave and convex slopes. The other slope shapes (flat) indicate negative value. Therefore, there is no indication that these shapes favor instability. The NDVI factor shows that the range between 0.05–0.1 and <-0.001 is relatively favorable (high susceptible) for landslide occurrence. It can be said that there is a diverse effect of the presence of vegetation to slope instability. In the case of land use, positive value of SI is seen on range land area only. This type of land use covers almost 90.5 % of study area. When comparing the relationship between landslides and lithology, the statistical values were positive in groups 3, 5, 7, and 8. Meanwhile, group 7 is very susceptible to landslide occurrence with value of 0.86; because of lithological formations are basic marl, marly limestone, siltstone, shale, and clay. In regarding distance from rivers, distances between 100–200 and 200–300 m have a positive value of SI (0.12 and 0.31, respectively), indicating a very high probability of landslide occurrence. Proximity from roads has little impact on landsliding. Distances between <100 m and 100–200 from roads show a very low or non-susceptible to landsliding compared to the other classes. On the other hand, three classes of proximity to roads show strong favor for landsliding. These classes are 200–300 m (SI = 0.06), 300–400 m (SI = 0.16), and >400 m (SI = 0.13). Maybe this appears to go against the visible pattern of more failures close to roads, it is likely due to a few large landslides where no roads are present. As a result, the large slides increase the percentage of landslide pixels occurring far from roads. In case of distance from faults, the intervals 600–200 and >800 m have weights (SI) of 0.21 and 0.08, respectively. It can be observed that as the

distance from faults increases, the landslide frequency generally decreases. We think this is for hard and very susceptible lithological formations in close and faraway of faults in study area. The drainage density <0.0018 km/km^2 has a SI value of 0.20, whereas class of 0.0027–0.013 has a SI value of −0.69. It can be observed that as the drainage density increases, the landslide frequency generally decreases. The relation between stream power index and landslide probabilities showed that class of 600–900 has the highest value of SI (0.37), and for compound topographic index, the class of 8–10 shows a high SI value (0.223). Similarly, for slope-length, the highest SI value was obtained for the interval of 60–90. The mentioned results for secondary topographic attributes (SPI, CTI, and LS) showed that these classes are very susceptible to landslide and its occurrence.

Finally, Landslide susceptibility map by statistical index (SI) model was created by following equation:

$$\begin{aligned} \mathrm{LSM_{SI}} = {} & ((W_{\mathrm{SI}}\text{slope degree}) + (W_{\mathrm{SI}}\text{slope aspect}) + (W_{\mathrm{SI}}\text{altitude}) \\ & + (W_{\mathrm{SI}}\text{plan curvature}) + (W_{\mathrm{SI}}\text{NDVI}) + (W_{\mathrm{SI}}\text{land use}) + (W_{\mathrm{SI}}\text{lithology}) \\ & + (W_{\mathrm{SI}}\text{distance from rivers}) + (W_{\mathrm{SI}}\text{distance from faults}) \\ & + (W_{\mathrm{SI}}\text{distance from roads}) + (W_{\mathrm{SI}}\text{SPI}) + (W_{\mathrm{SI}}\text{LS})) \end{aligned} \tag{13}$$

In this research, three landslide susceptibility maps such as binary logistic regression, analytical hierarchy process, and statistical index (Fig. 6a–c) were prepared in ArcGIS into four classes and according to natural break classification method (Falaschi et al. 2009; Bednarik et al. 2010; Erner et al. 2010; Constantin et al. 2011; Xu et al. 2012a, b, Xu and Xu 2012; Pourghasemi et al. 2012b, c, d).

6 Verification of the landslide susceptibility maps

To determine the accuracy of three landslide susceptibility models (Binary logistic regression, analytical hierarchy process, and statistical index) used in this study, two verification methods, the relative operating characteristics (ROC) and frequency ratio plot, were used. ROC curve analysis is a common method to assess the accuracy of a diagnostic test (Egan 1975). The ROC curve is a graphical representation of the trade-off between the false-negative and false-positive rates for every possible cutoff value. By tradition, the plot shows the false-positive rate (FPR) on the X axis (Eq. 14) and the true-positive rate (TPR) on the Y axis (Eq. 15).

$$X = \mathrm{FPR} = 1 - \left[\frac{\mathrm{TN}}{\mathrm{TN} + \mathrm{FP}}\right] \tag{14}$$

$$Y = \mathrm{TPR} = \left[\frac{\mathrm{TP}}{\mathrm{TP} + \mathrm{FN}}\right] \tag{15}$$

The area under the ROC curve (AUC) characterizes the quality of a forecast system by describing the system's ability to anticipate the correct occurrence or non-occurrence of pre-defined "events." The best method has a curve with the largest AUC; the AUC varies from 0.5 to 1.0. If the model does not predict the occurrence of the landslide any better than chance, the AUC would equal 0.5. A ROC curve of 1 represents perfect prediction. The quantitative–qualitative relationship between AUC and prediction accuracy can be classified as follows: 0.9–1, excellent; 0.8–0.9, very good; 0.7–0.8, good; 0.6–0.7, average; and 0.5–0.6, poor (Yesilnacar 2005). The AUC values of the ROC curve for BLR, AHP, and SI models were found to be 0.8520, 0.8037, and 0.7570, respectively (Fig. 7). Hence, it is

concluded that the binary logistic regression model employed in this study showed reasonably very good accuracy in predicting the landslide susceptibility of study area.

Also, the landslide susceptibility analyses were validated using frequency ratio plot. Due to, all of the landslide grid cells were overlaid on landslide susceptibility zones (low, moderate, high, and very high) in GIS, and frequency ratio was calculated for each of the susceptibility zones (Pourghasemi et al. 2012d). In an ideal landslide susceptibility map, the frequency ratio value is increasing from a low to a very high susceptibility zones (Pradhan and Lee 2010a, b; Pourghasemi et al. 2012c). A plot of the frequency ratio for the four landslide susceptibility classes of the three landslide susceptibility models is shown in Fig. 8. The results showed that the frequency ratio is gradually increased from the low to the very high susceptibility zone in the study area.

7 Discussion and conclusion

Landslide susceptibility maps provide fundamental knowledge of the causes and effective factors on landslide occurrence and can be effective in hazard management and its mitigation measures. In present research, we attempt to compare the results of landslide susceptibility mapping using of three different models namely: BLR, ST, and AHP in the north of Tehran metropolitan, Iran. Of total 528 identified landslide locations in the study area, 370 (70 %) were used as training data and the remaining 158 (30 %) were used for validation goals. In order to landslide susceptibility zonation, twelve conditioning factors such as slope degree, slope aspect, altitude, plan curvature, normalized difference vegetation index, land use, lithology, distance from rivers, distance from roads, distance from faults, stream power index, and slope-length were considered. For validation of generated landslide susceptibility maps in ArcGIS, the receiver operating characteristic (ROC) curves and frequency ratio plot were used.

According to obtained area under the curve (AUC), the binary logistic regression model has higher prediction performance (85.20 %) than statistical index (80.37 %) and analytical hierarchy process (75.70 %) models. Also the results of frequency ratio plot showed that the frequency ratio value is gradually increased from the low to the very high susceptibility zone in the study area, while this was validated our results.

Meanwhile, several investigators found overall accuracy rate relatively similar in some models such as FR, AHP, LR, and ANN (Jin et al. 2010; Park et al. 2012); conditional probability (CP), LR, ANN, and SVM (Yilmaz 2010); MCDA, SVM, and LR (Kavzoglu et al. 2013); heuristic and bivariate statistical models (Bijukchhen et al. 2012); probabilistic, bivariate and multivariate models (Pradhan and Youssef 2010; Tien Bui et al. 2011a; Kevin et al. 2011; Ozdemir and Altural 2012; Shahabi et al. 2012). On the other words, Ayalew et al. (2005), Esmali Ouri and Amirian (2009) stated that AHP model was better that the logistic regression in Sado Island, Japan and Iran, respectively. Yalcin (2008) reported AHP method gave a more realistic landslide susceptibility map than the bivariate statistical models (Wi and Wf). In another research, Yalcin et al. (2011) in order to landslide susceptibility mapping used of frequency ratio, AHP, bivariate statistics, and logistic regression in Trabzon, NE Turkey. They found that the weighting factor (Wf) method is better in prediction than the frequency ratio model, AHP, the statistical index (Wi), and logistic regression model.

Vahidnia et al. (2009) due to landslide hazard calculation in Mazandaran Province, Iran, used of four models namely: weights of evidence (WoE), AHP, ANN, and generalized linear regression (GLM). The estimated accuracy ranges from 80 to 88 %. It is then

inferred that the application of WoE in rating maps' categories and ANN to weight effective factors results in the maximum accuracy.

The main advantage of logistic regression over simple multiple regressions is that LR allows the use of binary dependent variable types in landslide susceptibility mapping. Although logistic regression is a commonly applied quantitative susceptibility mapping method, it has a major limitation of yielding average parameters for the study area (Fotheringham et al. 2001; Erner et al. 2010), which may differ locally in different parts of the study area.

van Westen et al. (2003) stated that the bivariate statistical method gives a satisfactory combination of the (subjective) professional direct mapping and the (objective) data driven analytical capabilities of a GIS. The main advantage of bivariate statistical procedures is that the professional, who executes the analysis, determines the factors or combinations of factors used in the assessment. This enables the introduction of expert opinion into the process. Bivariate statistics are a useful tool in the assessment of landslide susceptibility, but can best be used as a supporting tool to make quantitative estimations of the importance of the various factors involved.

The general purpose of the AHP is to support the decision makers in selecting the best alternative from the various possible choice alternatives under the presence of multiple priorities (Jankowski 1995). On the other hand, AHP model is conventionally based on a rating system provided by expert opinion. In fact, expert opinion is very useful in solving complex problems like landslides. However, to some extent, opinions may change for every individual expert and thus may be subjected to cognitive limitations with uncertainty and subjectivity. Another aspect is that data driven methods are also powerful in landslide susceptibility mapping and contain less subjectivity. Therefore, it is important to analyze the spatial relationship between the landslide conditioning factors and landslide locations. The statistical-based models (Bivariate and multivariate) allow users to order parametric importance before the landslide susceptibility analyses application.

As a final conclusion, these maps can provide very useful information for planners, decision makers, and engineers in slope management and land use planning in landslide areas, and we believe that the results obtained from our study provide a considerable contribution to the landslide literature.

Acknowledgments The authors gratefully acknowledge of National Geographic Organization (NGO) (http://www.ngo-iran.ir/ngo.htm) for providing the satellite images (IRS). This research was carried out as part of the first author's PhD thesis at the watershed management engineering, Tarbiat Modares University (TMU), Mazandaran, Iran. Also, the authors would like to thank two anonymous reviewers and editor for their helpful comments on the previous version of the manuscript.

References

Akgun A, Turk N (2010) Landslide susceptibility mapping for Ayvalik (Western Turkey) and its vicinity by multi-criteria decision analysis. Environ Earth Sci 61:595–611

Akgun A, Sezer EA, Nefeslioglu HA, Gokceoglu C, Pradhan B (2012) An easy-to-use MATLAB program (MamLand) for the assessment of landslide susceptibility using a Mamdani fuzzy algorithm. Comput Geosci 38(1):23–34

Aleotti P, Chowdhury R (1999) Landslide hazard assessment: summary review and new perspectives. Bull Eng Geol Environ 58:21–44

Atkinson PM, Massari R (1998) Generalized linear modelling of susceptibility to landsliding in the central Appennines, Italy. Comput Geosci 24(4):373–385

Ayalew L, Yamagishi H (2005) The application of GIS-based logistic regression for landslide susceptibility mapping in the Kakuda-Yahiko Mountains, Central Japan. Geomorphology 65(1–2):15–31
Ayalew L, Yamagishi H, Marui H, Kanno T (2005) Landslides in Sado Island of Japan: Part II. GIS-based susceptibility mapping with comparisons of results from two methods and verifications. Eng Geol 81:432–445
Bai S, Wang J, Lu G, Zhou P, Hou S, Xu S (2010) GIS-based logistic regression for landslide susceptibility mapping of the Zhongxian segment in the Three Gorges area, China. Geomorphology 115:23–31
Ballabio C, Sterlacchini S (2012) Support vector machines for landslide susceptibility mapping: the Staffora River Basin case study, Italy. Math Geosci 44:47–70
Barredo JI, Benavidesz A, Herh J, Van Westen CJ (2000) Comparing heuristic landslide hazard assessment techniques using GIS in the Tirajana basin, Gran Canaria Island, Spain. Int J Appl Earth Obs 2:9–23
Bednarik M, Magulova B, Matys M, Marschalko M (2010) Landslide susceptibility assessment of the Kralovany–Liptovsky Mikulas railway case study. Phys Chem Earth Parts A/B/C 35(3–5):162–171
Bijukchhen SM, Kayastha P, Dhital MR (2012) A comparative evaluation of heuristic and bivariate statistical modelling for landslide susceptibility mappings in Ghurmi–Dhad Khola, east Nepal. Arab J Geosci. doi:10.1007/s12517-012-0569-7
Carrara A, Cardinali M, Guzzetti F, Reichenbach P (1995) GIS technology in mapping landslide hazard. Geographical information systems in assessing natural hazards. Kluwer Academic Publishers, Dordrecht, pp 135–175
Cevik E, Topal T (2003) GIS-based landslide susceptibility mapping for a problematic segment of the natural gas pipeline, Hendek (Turkey). Environ Geol 44:949–962
Chen Y, Yu J, Shahbaz K, Xevi E (2009) A GIS-based sensitivity analysis of multi-criteria weights. In: Proceedings of the 18th World IMACS/MODSIM Congress, Cairns, Australia 13–17 July 2009. http://mssanz.org.au/modsim09
Constantin M, Bednarik M, Jurchescu MC, Vlaicu M (2011) Landslide susceptibility assessment using the bivariate statistical analysis and the index of entropy in the Sibiciu Basin (Romania). Environ Earth Sci 63:397–406
CRED (2009) Centre for Research on the Epidemiology of Disasters (CRED) website. http://www.dmdat.be/
Dahal RK, Hasegawa S, Nonomura A, Yamanaka M, Takuro M, Nishino K (2008) GIS-based weights-of-evidence modelling of rainfall-induced landslides in small catchments for landslide susceptibility mapping. Environ Geol 54:311–324
Demir G, Aytekin M, Akgun A, Ikizler SB, Tatar O (2012) A comparison of landslide susceptibility mapping of the eastern part of the North Anatolian Fault Zone (Turkey) by likelihood-frequency ratio and analytic hierarchy process methods. Nat Hazards. doi:10.1007/s11069-012-0418-8
Devkota KC, Regmi AD, Pourghasemi HR, Yoshida K, Pradhan B, Ryu IC, Dhital MR, Althuwaynee OF (2013) Landslide susceptibility mapping using certainty factor, index of entropy and logistic regression models in GIS and their comparison at Mugling-Narayanghat road section in Nepal Himalaya. Nat Hazards 65:135–165
ECInc (Expert Choice Inc.) (1995) Decision support software: tutorial, expert choice, Student Version 9. Expert Choice Inc., Pittsburgh
Egan JP (1975) Signal detection theory and ROC analysis. NY: Acad 195:266–268
Ercanoglu M, Gokceoglu C (2004) Use of fuzzy relations to produce landslide susceptibility map of a landslide prone area (West Black Sea Region, Turkey). Eng Geol 75:229–250
Ercanoğlu M, Temiz FA (2011) Application of logistic regression and fuzzy operators to landslide susceptibility assessment in Azdavay (Kastamonu, Turkey). Environ Earth Sci 64:949–964
Erner A, Duzgun HSB (2012) Landslide susceptibility assessment: what are the effects of mapping unit and mapping method? Environ Earth Sci 66:859–877
Erner A, Sebnem H, Duzgun B (2010) Improvement of statistical landslide susceptibility mapping by using spatial and global regression methods in the case of More and Romsdal (Norway). Landslides 7:55–68
Esmali Ouri A, Amirian S (2009) Landslide hazard zonation using MR and AHP methods and GIS techniques in Langan watershed, Ardabil, Iran. International Conference on ACRS 2009, Beijing, China
Falaschi F, Giacomelli F, Federici PR, Puccinelli A, D'Amato Avanzi G, Pochini A, Ribolini A (2009) Logistic regression versus artificial neural networks: landslide susceptibility evaluation in a sample area of the Serchio River valley, Italy. Nat Hazards 50:551–569
Feizizadeh B, Blaschke T (2012a) Land suitability analysis for Tabriz County, Iran: a multi-criteria evaluation approach using GIS. J Environ Plan Manag. doi:10.1080/09640568.2011.646964
Feizizadeh B, Blaschke T (2012b) GIS-Multi-criteria Decision Analysis for landslide susceptibility mapping: comparing three methods for the Urmia lake basin, Iran. Nat Hazards. doi:10.1007/s11069-012-0463-3

Fotheringham AS, Charlton ME, Brunsdon C (2001) Spatial variations in school performance: a local analysis using geographically weighted regression. Geogr Environ Model 5:43–66
Garcia-Rodriguez MJ, Malpica JA, Benito B, Diaz M (2008) Susceptibility assessment of earthquake-triggered landslides in El Salvador using logistic regression. Geomorphology 95:172–191
Geology Survey of Iran (GSI) (1997) http://www.gsi.ir/Main/Lang_en/index.html
Ghosh S (2011) Knowledge guided empirical prediction of landslide hazard, a dissertation to obtain the degree of doctor at the University of Twente, p 214
Guzzetti F, Carrarra A, Cardinali M, Reichenbach P (1999) Landslide hazard evaluation: a review of current techniques and their application in a multi-scale study, Central Italy. Geomorphology 31:81–216
Guzzetti F, Cardinali M, Reichenbach P, Carrara A (2000) Comparing landslide maps: a case study in the upper Tiber River Basin, central Italy. Environ Manag 25(3):247–363
Guzzetti F (2005) Landslide hazard and risk assessment. PhD Dissertation, Rheinischen Friedrich-Wilhelms-University Bonn, 389pp
Hall FG, Townshend JR, Engman ET (1995) Status of remote sensing algorithms for estimation of land surface state parameters. Remote Sens Environ 51:138–156. doi:10.1016/0034-4257
Hasekiogullari GD, Ercanoglu M (2012) A new approach to use AHP in landslide susceptibility mapping: a case study at Yenice (Karabuk, NW Turkey). Nat Hazards 63(2):1157–1179
Hengl T, Gruber S, Shrestha DP (2003) Digital terrain analysis in ILWIS. International Institute for Geo-Information Science and Earth Observation Enschede, The Netherlands, p 62
Jankowski P (1995) Integrating geographical information systems and multiple criteria decision-making methods. Int J Geogr Inf Sci 9:251–273
Jin GC, Che OhY, Choi CU (2010) The comparative research of landslide susceptibility mapping using FR, AHP, LR, ANN. Korean Soc Geosp Inf Syst 9:13–20
Kavzoglu T, Sahin EK, Colkesen I (2013) Landslide susceptibility mapping using GIS-based multi-criteria decision analysis, support vector machines, and logistic regression. Landslides. doi:10.1007/s10346-013-0391-7
Kevin LKW, Tay LT, Lateh H (2011) Landslide hazard mapping of Penang Island using probabilistic methods and logistic regression. Imaging Systems and Techniques (IST), 2011 IEEE International Conference, pp 273–278
Kheirkhah Zarkesh MM (2005) Decision support system for floodwater spreading site selection in Iran. Thesis to fulfil the requirements for the degree of Doctor on the authority of the rector magnificus of Wageningen University, p 259
Komac M (2006) A landslide susceptibility model using the analytical hierarchy process method and multivariate statistics in perialpine Slovenia. Geomorphology 74:17–28
Lee S (2005) Application of logistic regression model and its validation for landslide susceptibility mapping using GIS and remote sensing data. Int J Remote Sens 26:1477–1491
Lee S, Pradhan B (2006) Probabilistic landslide hazards and risk mapping on Penang Island, Malaysia. J Earth Syst Sci 115:661–672
Lee S, Pradhan B (2007) Landslide hazard mapping at Selangor, Malaysia using frequency ratio and logistic regression models. Landslides 4:33–41
Lee S, Ryu JH, Won JS, Park HJ (2004) Determination and application of the weights for landslide susceptibility mapping using an artificial neural network. Eng Geol 71:289–302
Li C, Ma T, Sun L, Li W, Zheng A (2011) Application and verification of fractal approach to landslide susceptibility mapping. Natl Hazards. doi:10.1007/s11069-011-9804-x
Majtan S, Omura H, Morita K (2002) Fractal dimension as an indicator of probability for landslides in North Matsuura, Japan. Geografický Casopis 54(1):5–19
Malczewski J (1999) GIS and multi-criteria decision analysis. Wiley, New York, p 392
Marjanović M, Kovačević M, Bajat B, Voženílek V (2011) Landslide susceptibility assessment using SVM machine learning algorithm. Eng Geol 123:225–234
Miller DJ, Sias J (1998) Deciphering large landslides: linking hydrologic, groundwater, and slope-stability model through GIS. Hydro Process 12(6):924–942
Mohammady M, Pourghasemi HR, Pradhan B (2012) Landslide susceptibility mapping at Golestan Province, Iran: a comparison between frequency ratio, Dempster-Shafer, and weights-of-evidence models. J Asian Earth Sci 61:221–236
Moore ID, Burch GJ (1986) Sediment transport capacity of sheet and rill flow: application of unit stream power theory. Water Res 22:1350–1360
Moore ID, Wilson JP (1992) Length-slope factors for the revised universal soil loss equation: simplified method of estimation. J Soil Water Conserv 47:423–428
Moore ID, Grayson RB, Ladson AR (1991) Digital terrain modeling: a review of hydrological, geomorphological, and biological applications. Hydro Process 5:3–30

Nandi A, Shakoor A (2010) A GIS-based landslide susceptibility evaluation using bivariate and multivariate statistical analyses. Eng Geol 110:11–20

Nefeslioglu HA, Gokceoglu C, Sonmez H (2008) An assessment on the use of logistic regression and artificial neural networks with different sampling strategies for the preparation of landslide susceptibility maps. Eng Geol 97:171–191

Nefeslioglu HA, Sezer E, Gökçeoğlu C, Bozkır AS, Duman TY (2010) Assessment of landslide susceptibility by decision trees in the metropolitan area of Istanbul, Turkey. Math Probl in Eng, 2010, Article ID: 901095

Nie HF, Diao SJ, Liu JX, Huang H (2001) The application of remote sensing technique and AHP-fuzzy method in comprehensive analysis and assessment for regional stability of Chongqing City, China. In: Proceedings of the 22nd international Asian Conference on Remote Sensing, vol 1, pp 660–665

O'Brien RM (2007) A caution regarding rules of thumb for variance inflation factors. Qual Quant 41(5):673–690

Oh HJ, Lee S (2010) Cross-validation of logistic regression model for landslide susceptibility mapping at Geneoung areas, Korea. Disaster Adv 3:44–55

Oh HJ, Lee S (2011) Landslide susceptibility mapping on Panaon Island, Philippines using a geographic information system. Environ Earth Sci 62:935–951

Oh HJ, Pradhan B (2011) Application of a neuro-fuzzy model to landslide susceptibility mapping for shallow landslides in a tropical hilly area. Comput Geosci 37(9):1264–1276. doi:10.1016/j.cageo.2010.10.012

Oh HJ, Lee S, Chotikasathien W, Kim CH, Kwon JH (2009) Predictive landslide susceptibility mapping using spatial information in the Pechabun area of Thailand. Environ Geol 57:641–651

Ohlmacher CG, Davis CJ (2003) Using multiple regression and GIS technology to predict landslide hazard in northeast Kansas, USA. Eng Geol 69:331–343

Ozdemir A (2009) Landslide susceptibility mapping of vicinity of Yaka Landslide (Gelendost, Turkey) using conditional probability approach in GIS. Environ Geol 57:1675–1686

Ozdemir A (2011) Using a binary logistic regression method and GIS for evaluating and mapping the groundwater spring potential in the Sultan Mountains (Aksehir, Turkey). J Hydrol 405:123–136

Ozdemir A, Altural T (2012) A comparative study of frequency ratio, weights of evidence and logistic regression methods for landslide susceptibility mapping: Sultan Mountains, SW Turkey. J Asian Earth Sci. doi:10.1016/j.jseaes.2012.12.014

Park S, Choi C, Kim B, Kim J (2012) Landslide susceptibility mapping using frequency ratio, analytic hierarchy process, logistic regression, and artificial neural network methods at the Inje area, Korea. Environ Earth Sci. doi:10.1007/s12665-012-1842-5

Pourghasemi HR, Pradhan B, Gokceoglu C, Mohammadi M, Moradi HR (2012a) Application of weights-of evidence and certainty factor models and their comparison in landslide susceptibility mapping at Haraz watershed, Iran. Arab J Geosci. doi:10.1007/s12517-012-0532-7

Pourghasemi HR, Pradhan B, Gokceoglu C, Deylami Moezzi K (2012b) A comparative assessment of prediction capabilities of Dempster-Shafer and Weights-of-evidence models in landslide susceptibility mapping using GIS. Geomat Natl Hazards Risk. doi:10.1080/19475705.2012.662915

Pourghasemi HR, Pradhan B, Gokceoglu C (2012c) Application of fuzzy logic and analytical hierarchy process (AHP) to landslide susceptibility mapping at Haraz watershed, Iran. Nat Hazards 63(2):965–996

Pourghasemi HR, Mohammady M, Pradhan B (2012d) Landslide susceptibility mapping using index of entropy and conditional probability models in GIS: Safarood Basin, Iran. Catena 97:71–84

Pourghasemi HR, Gokceoglu C, Pradhan B, Deylami Moezzi K (2012e) Landslide susceptibility mapping using a spatial multi criteria evaluation model at Haraz Watershed, Iran. In: Pradhan B, Buchroithner M (eds) Terrigenous mass movements. Springer, Berlin, pp 23–49. doi:10.1007/978-3-642-25495-6-2

Pourghasemi HR, Pradhan B, Gokceoglu C (2012f) Remote sensing data derived parameters and its use in landslide susceptibility assessment using Shannon's entropy and GIS, AEROTECH IV–2012, Kuala Lumpur, Malaysia. Appl Mech Mater 225:486–491. doi:10.4028/www.scientific.net/AMM.225.486

Pourghasemi HR, Goli Jirandeh A, Pradhan B, Xu C, Gokceoglu C (2013) Landslide susceptibility mapping using support vector machine and GIS. J Earth Syst Sci 122(2):349–369

Pradhan B (2010a) Application of an advanced fuzzy logic model for landslide susceptibility analysis. Int J Comput Intell Syst 3(3):370–381

Pradhan B (2010b) Landslide susceptibility mapping of a catchment area using frequency ratio, fuzzy logic and multivariate logistic regression approaches. J Indian Soc Remote Sens 38(2):301–320

Pradhan B (2011a) Manifestation of an advanced fuzzy logic model coupled with geo-information techniques for landslide susceptibility analysis. Environ Ecol Stat 18(3):471–493

Pradhan B (2011b) Use of GIS-based fuzzy logic relations and its cross application to produce landslide susceptibility maps in three test areas in Malaysia. Environ Earth Sci 63(2):329–349
Pradhan B (2013) A comparative study on the predictive ability of the decision tree, support vector machine and neuro-fuzzy models in landslide susceptibility mapping using GIS. Comput Geosci 51:350–365
Pradhan B, Buchroithner MF (2010) Comparison and validation of landslide susceptibility maps using an artificial neural network model for three test areas in Malaysia. Environ Eng Geosci 16(2):107–126
Pradhan B, Lee S (2010a) Delineation of landslide hazard areas using frequency ratio, logistic regression and artificial neural network model at Penang Island, Malaysia. Environ Earth Sci 60:1037–1054
Pradhan B, Lee S (2010b) Landslide susceptibility assessment and factor effect analysis: back-propagation artificial neural networks and their comparison with frequency ratio and bivariate logistic regression modeling. Environ Model Softw 25(6):747–759
Pradhan B, Youssef AM (2010) Manifestation of remote sensing data and GIS on landslide hazard analysis using spatial-based statistical models. Arab J Geosci 3:319–326
Raman R, Punia M (2012) The application of GIS-based bivariate statistical methods for landslide hazards assessment in the upper Tons river valley, Western Himalaya, India. Georisk Assess Manag Risk Eng Syst Geohazards 6(3):145–161
Rautela P, Lakhera RC (2000) Landslide risk analysis between Giri and Tons Rivers in Himachal Himalaya (India). Int J Appl Earth Obs Geoinf 2:153–160
Regmi AD, Yoshida K, Pradhan B, Pourghasemi HR, Khumamoto T, Akgun A (2013) Application of frequency ratio, statistical index and weights-of-evidence models, and their comparison in landslide susceptibility mapping in Central Nepal Himalaya. Arab J Geosci. doi:10.1007/s12517-012-0807-z
Rozos D, Pyrgiotis L, Skias S, Tsagaratos P (2008) An implementation of rock engineering system for ranking the instability potential of natural slopes in Greek territory, an application in Karditsa County. Landslides 5:261–270
Saaty TL (1977) A scaling method for priorities in hierarchical structures. J Math Psychol 15:234–281
Saaty T (1980) The analytical hierarchy process. McGraw-Hill, New York
Saaty TL (1994) Fundamentals of decision making and priority theory with analytic hierarchy process. RWS Publications, Pittsburgh, p 527
Saaty TL (2008) Decision making with the analytic hierarchy process. Int J Serv Sci 1(1):83–98
Schumacher M, Robner R, Vach W (1996) Neural networks and logistic regression: Part 1. Comput Stat Data Anal 21:661–682
Sezer EA, Pradhan B, Gokceoglu C (2011) Manifestation of an adaptive neuro-fuzzy model on landslide susceptibility mapping: Klang valley, Malaysia. Expert Syst Appl 38(7):8208–8219
Shahabi H, Ahmad BB, Khezri S (2012) Evaluation and comparison of bivariate and multivariate statistical methods for landslide susceptibility mapping (case study: Zab basin). Arab J Geosci. doi:10.1007/s12517-012-0650-2
Sidle RC, Ochiai H (2006) Landslides: processes, prediction, and landuse. American Geophysical Union, Washington, D.C. Water Res Monograph 18, p 312
Soeters R, Van Westen CJ (1996) Slope instability recognition analysis and zonation. In: Turner KT, Schuster RL (eds) Landslide: investigation and mitigation. Spec Rep 47. Transportation Research Board, National Research Council, Washington, DC, pp 129–177
Song Y, Gong J, Gao S, Wang D, Cui T, Li Y, Wei B (2012) Susceptibility assessment of earthquake-induced landslides using Bayesian network: a case study in Beichuan, China. Comput Geosci 42:189–199
Tien Bui D, Lofman O, Revhaug I, Dick O (2011a) Landslide susceptibility analysis in the Hoa Binh province of Vietnam using statistical index and logistic regression. Nat Hazards 59:1413–1444
Tien Bui D, Pradhan B, Lofman O, Revhaug I, Dick OB (2011b) Landslide susceptibility mapping at Hoa Binh province (Vietnam) using an adaptive neuro fuzzy inference system and GIS. Comput Geosci. doi:10.1016/j.cageo.2011.10.031
Tien Bui D, Pradhan B, Lofman O, Revhaug I (2012) Landslide susceptibility assessment in Vietnam using support vector machines, decision tree and Naïve Bayes models. Math Probl Eng 2012:1–26. doi:10.1155/2012/974638
Vahidnia MH, Alesheikh AA, Alimohammadi A, Hosseinali F (2009) Landslide hazard zonation using quantitative methods in GIS. Int J Civil Eng 7(3):176–189
Vahidnia MH, Alesheikh AA, Alimohammadi A, Hosseinali F (2010) A GIS based neuro fuzzy procedure for integrating knowledge and data in landslide susceptibility mapping. Comput Geosci 36(9):1101–1114
van Westen C (1997) Statistical landslide hazard analysis. ILWIS 2.1 for Windows application guide. ITC Publication, Enschede, pp 73–84

van Westen CJ, Rengers N, Terlien MTJ, Soeters R (1997) Prediction of the occurrence of slope instability phenomena through GIS-based hazard zonation. Geol Rundsch 86(2):404–414
van Westen CJ, Rengers N, Soeters R (2003) Use of geomorphological information in indirect landslide susceptibility assessment. Nat Hazards 30:399–419
van Westen CJ, Asch TWJ, Soeters R (2006) Landslide hazard and risk zonation-why is it still so difficult? Bull Eng Geol Environ 65:67–184
Vargas LG (1990) An overview of the analytic hierarchy process and its applications. Eur J Oper Res 48:2–8
Varnes DJ (1978) Slope movement types and processes. In: Schuster RL, Krizek RJ (eds) Landslides analysis and control. Special report, vol 176. Transportation Research Board, National Academy of Sciences, New York, pp 11–33
Varnes DJ (1984) With IAEG commission on landslides and other mass movements: landslide hazard zonations: a review of principles and practices. UNESCO, Paris, p 63
Wan S (2012) Entropy-based particle swarm optimization with clustering analysis on landslide susceptibility mapping. Environ Earth Sci. doi:10.1007/s12665-012-1832-7
Xu C, Xu X (2012) Controlling parameter analyses and hazard mapping for earthquake-triggered landslides: an example from a square region in Beichuan County, Sichuan Province, China. Arab J Geosci. doi:10.1007/s12517-012-0646-y
Xu C, Xu X, Dai F, Xiao J (2012a) Landslide hazard mapping using GIS and weight of evidence model in Qingshui River watershed of 2008 Wenchuan earthquake struck region. J Earth Sci 23(1):97–120
Xu C, Dai F, Xu X, Lee YH (2012b) GIS-based support vector machine modeling of earthquake-triggered landslide susceptibility in the Jianjiang River watershed, China. Geomorphology 145–146:70–80
Xu C, Xu X, Lee YH, Tan X, Yu G, Dai F (2012c) The 2010 Yushu earthquake triggered landslide hazard mapping using GIS and weight of evidence modeling. Environ Earth Sci 66(6):1603–1616
Yalcin A (2008) GIS-based landslide susceptibility mapping using analytical hierarchy process and bivariate statistics in Ardesen (Turkey): comparisons of results and confirmations. Catena 72:1–12
Yalcin A, Reis S, Aydinoglu AC, Yomralioglu T (2011) A GIS-based comparative study of frequency ratio, analytical hierarchy process, bivariate statistics and logistics regression methods for landslide susceptibility mapping in Trabzon, NE Turkey. Catena 85:274–287
Yang Z, Lee YH (2006) The fractal characteristics of landslides induced by earthquakes and rainfall in central Taiwan, The Geological Society of London, pp 1–8
Yao X, Tham LG, Dai FC (2008) Landslide susceptibility mapping based on support vector machine: a case study on natural slopes of Hong Kong, China. Geomorphology 101(4):572–582
Yesilnacar EK (2005) The application of computational intelligence to landslide susceptibility mapping in Turkey, Ph.D Thesis. Department of Geomatics the University of Melbourne, p 423
Yilmaz I (2009) Landslide susceptibility mapping using frequency ratio, logistic regression, artificial neural networks and their comparison: a case study from Kat landslides (Tokat-Turkey). Comput Geosci 35:1125–1138
Yilmaz I (2010) Comparison of landslide susceptibility mapping methodologies for Koyulhisar, Turkey: conditional probability, logistic regression, artificial neural networks, and support vector machine. Environ Earth Sci 61:821–836
Zare M, Pourghasemi HR, Vafakhah M, Pradhan B (2012) Landslide susceptibility mapping at Vaz watershed (Iran) using an artificial neural network model: a comparison between multi-layer perceptron (MLP) and radial basic function (RBF) algorithms. Arab J Geosci. doi:10.1007/s12517-012-0610-x